Separation in Slightly Viscous Flow

Johan Hoffman and Claes Johnson

July 12, 2011

Abstract

We present a scenario for separation in slightly viscous incompressible turbulent flow around a solid body supported by computation, mathematical analysis and experimental observation, which is fundamentally different from the scenario for viscous laminar flow by Prandtl based on adverse pressure gradients retarding the flow to stagnation at separation. We make a distinction betweeen separation from a laminar boundary layer with no-slip boundary condition and a turbulent boundary layer with slip. We note that separation occurs if $\frac{\partial p}{\partial n} < \frac{U^2}{R}$, where $\frac{\partial p}{\partial n}$ is the pressure gradient normal to the boundary into the fluid, U is a flow speed close to the boundary and R the curvature of the boundary, positive for a convex body. We note that in a laminar boundary layer $\frac{\partial p}{\partial n} > 0$ only in contracting flow, which causes separation as soon as the flow expands after the crest of the body. We observe that in a turbulent boundary layer with slip, $\frac{\partial p}{\partial n} > 0$ is possible also in expanding flow which can delay separation. We present a basic mechanism for tangential separation with slip based on instability at rear points of stagnation generating low-pressure rolls of streamwise vorticity reducing $\frac{\partial p}{\partial n}$. We present new explanations of the drag-reducing effect of the dimples of a golf ball, the Magnus effect, the reverse Magnus effect and the Coanda effect, all related to delayed separation from a turbulent boundary layer with slip.

1 Prandtl and Flow Separation

The problem of *fluid separation* is of fundamental importance in fluid mechanics, in particular in the case of a *slightly viscous incompressible* flow in aero/hydro mechanics considered in this note. As a body moves through a slightly viscous fluid initially at rest, like a car or airplane moving through still air, or equivalently as a fluid flows around a body at rest, approaching fluid particles are deviated by the body in *contracting flow*, switching to *expanding flow* at a *crest* and eventually *separate* away from the body somewhere in the rear, at or after the crest. In the front the flow is typically *laminar* and approaches/*attaches* to the boundary at *stagnation* with zero fluid velocity. On the other hand, the fluid mechanics of the *turbulent separation* occuring in the rear in slightly viscous flow, which creates *drag* and *lift* forces, appears to be largely unknown, despite its crucial importance in many applications, including flying and sailing. The purpose of this article is to contribute to fill this gap. We focus here on the basic case of turbulent separation from a convex body like a sphere, circular cylinder, wing, car or boat hull.

In 1904 the young German physicist Ludwig Prandtl (1875-1953) suggested in a 10 page sketchy presentation entitled *Motion of Fluids with Very Little Viscosity* [22] at the Third International Congress of Mathematics in Heidelberg, that the substantial drag of a bluff body moving through a fluid with very small viscosity (such as air or water), possibly could arise from the presence of of a thin *laminar boundary layer* causing the flow to *separate* from the boundary brought to stagnation under an *adverse pressure gradient* (negative pressure gradient in the flow direction), to form a low-pressure wake behind the body. Prandtl's boundary layer has a distinctive two-dimensional (2d) character with the flow changing slowly in the direction transverse to the flow and parallel to the boundary. The acceptance of Prandtl's ideas was remarkably slow [1]:

- *Prandtls idea (about the boundary layer) went virtually unnoticed by anybody outside of Göttingen... The fifth and sixth editions of Lambs classic text Hydrodynamics published in 1924, devoted only one paragraph to the boundary-layer concept.*

However, Prandtl got two forceful students, Theodore von Karman (emigrated to the US in 1930) and Hermann Schlichting (remained in Germany), who crowned Prandtl as the *father of modern fluid mechanics*. Prandtl's main ideas are described as follows in Schlichting's treatise *Boundary Layer Theory* from 1951:

- *Boundary layer flow has the peculiar property that under certain conditions the flow in the immediate neighbourhood of a solid wall becomes reversed causing the boundary layer to separate from it. This is accompanied by a more or less pronounced formation of eddies in the wake of the body. Thus the pressure distribution is changed and differs markedly from that in a frictionless stream. The deviation in pressure distribution from that of the ideal is the cause of form drag, and its calculation is thus made possible with the aid of boundary layer theory.*

- *The first important question to answer is to find when separation of the flow from the wall may occur. When a region with an adverse pressure gradient exists along the wall, the retarded fluid particles cannot, in general, penetrate too far into the region of increased pressure owing to their small kinetic energy. Thus the boundary layer is deflected sideways from the wall, separates from it, and moves into the main stream. In general the fluid particles follow the pressure gradient and move in a direction opposite to the external stream.*

- *In some cases the boundary layer increases its thickness considerably in the downstream direction and the flow in the boundary layer becomes reversed. This causes the decelerated fluid particles to be forced outwards, which means that the boundary layer is separated from the wall. We then speak of boundary layer separation. This phenomenon is always associated with the formation of vortices and with large energy losses in the wake of the body. The large drag can be explained by the existence of large deviation in pressure distribution (from potential flow), which is a consequence of boundary-layer separation.*

- *Downstream the pressure minimum the discrepancies increase very fast on approaching the separation point (for circular cylinder).*

- *The circumstance that real flows can support considerable rates of pressure increase (adverse pressure gradients) in a large number of cases without separation is due to the fact that the flow is mostly turbulent. The best known examples include cases of flow past circular cylinders and spheres, when separation occurs much further upstream in laminar than in turbulent flow. It is nevertheless useful to consider laminar flow because it is much more amenable to mathematical treatment than is the case of turbulent flow....At the present time these very complicated phenomena (separation in turbulent flow) are far from being understood completely...*

- *The form drag which does not exist in frictionless subsonic flow, is due to the fact that the presence of the boundary layer modifies the pressure distribution on the body as compared with ideal flow, but its computation is very difficult.*

- *The origin of pressure drag lies in the fact that the boundary layer exerts a displacement action on the external stream. This modifies somewhat the pressure distribution on the body surface. In contrast with potential flow (d'Alembert's paradox), the resultant of this pressure distribution modified by friction no longer vanishes but produces a preessure drag which must be added to skin friction. The two together give form drag.*

- *In the case of the most important fluids, namely water and air, the viscosity is very small and, consequently, the forces due to viscous friction are, generally speaking, very small compared with the remaining forces (gravity and pressure forces). For this resaon it was very difficult to comprehend that very small frictional forces omitted in classical (inviscid) theory influenced the motion of a fluid to so large extent*.

Prandtl described the difficulties himself in *Applied Hydro- and Aeromechanics* from 1934:

- *Only in the case where the "boundary layer" formed under the influence of the viscosity remains in contact with the body, can an approximation of the actual fluid motion by means of a theory in terms of the ideal frictionsless fluid be attempted, whereas in all cases where the boundary leaves the body, a theoretical treatment leads to results which do not coincide at all with experiment. And it had to be confessed that the latter case occurs most frequently.*

In a nutshell, these quotes present much of the essence of modern fluid mechanics propagated in standard books and courses in fluid mechanics: Drag and lift in slightly viscous flow are claimed to arise from 2d separation in a thin viscous laminar boundary layer brought to stagnation with reversed flow due to an adverse pressure gradient. On the other hand, both Prandtl and Schlichting admit that this standard scenario does not describe turbulent flow, always arising in slightly viscous flow, but persists that *"it is nevertheless useful to consider laminar flow because it is much more amenable to mathematical treatment"*. However, turbulent and laminar flow have different properties, and drawing conclusions about turbulent flow from studies of laminar flow can be grossly misleading.

2 Critique by Lancaster and Birkhoff

Prandtl's contribution to fluid mechanics was to explain separation, drag and lift as effects of a very small (vanishingly small) viscosity. This view has been seriously questioned, however with little effect since no alternative to Prandtl's theory has been in sight. Lancaster stated already in 1907 in his in *Aerodynamics*[20]:

- *According to the mathematical theory of Euler and Lagrange, all bodies are of streamline form (with zero dragh and lift). This conclusion, which would otherwise constitute a reductio ad absurdum, is usually explained on the gorund the fluid of theory is inviscid, whereas real possess viscosity. It is questionable of this expanlanation alone is adequate.*

Birkhoff followed up in his *Hydromechanics* from 1950 [3]:

- *The art of knowing "how to apply" hydrodynamical theories can be learned even more effectively, in my opinion, by studying the paradoxes I will describe (e.g d'Alemberts paradox). Moreover, I think that to attribute them all to the neglect of viscosity is an oversimplification. The root lies deeper, in lack of precisely that deductive rigor whose importance is so commonly minimized by physicists and engineers.*

However, critique of Prandtl was not well received, as shown in the review of Birkhoff's book by James. J. Stoker [24]. The result is that Prandtl still dominates fluid mechanics today, although the belief in Prandtl's boundary layer theory (BLT) seems to be fading as expressed by Cowley [4]:

- *But is BLT a 20th century paradox? One may argue, yes, since for quantitative agreement with experiment BLT will be outgunned by computational fluid dynmaics in the 21st century.*

The 21st century is now here, and yes, computational fluid mechanics reveals a different scenario than Prandtl's.

But Prandtl's influence is still strong, as evidenced by the common belief that accurate computational simulation requires very thin boundary layers to be resolved. Thus Kim and Moin [19] claim in 200? that to correctly predict lift and drag of an aircraft at the relevant Reynolds number of size 10^8, requires computation on meshes with more than 10^{16} mesh points, which is way out of reach for any foreseeable computer, a conviction supported by Henningson [21] in 2008. This puts CFD into a deadlock: Either compute at irrelevant too small Reynolds numbers or invent turbulence models, which has shown to be very difficult.

Techniques for preventing 2d laminar separation based on suction and blowing have been suggested. In the recent study [25] computational simulations are presented of synthetic jet control for a NACA 0015 wing at Reynolds number 896.000 (based on the chord length) for different angles of attack. As indicated, the relevant Reynolds number is two orders of magnitude larger, and the relevance of the study can be questioned. The effects of the synthetic jet control may simply be overshadowed by turbulent boundary layers.

3 Outline

In this note we give evidence that Prandtl's boundary layer theory for 2d laminar separation has fallen into this trap, with the unfortunate result is that much research and effort has gone into preventing *2d laminar separation* in flows which effectively are turbulent with *3d turbulent separation*. We present a scenario for 3d turbulent separation with streamwise vorticity supported by analysis, computation and experiments, which connects to the familiar experience of the rotating flow through a bathtub drain replacing the theoretically possible but unstable fully radial flow. This new scenario is radically different from Prandtl's scenario for 2d laminar separation at stagnation (without streamwise vorticity). We shall find that Prandtl's 2d scenario is academic in the sense that laminar separation triggers turbulence which allows flow *reattachment* after a *separation bubble* into later 3d turbulent separation.

We show that 2d laminar separation with no-slip occurs at the crest of slightly vicous flow with a large wake and drag, while turbulent separation can occur after the crest with smaller wake and drag. We show that drag can be seen as cost of separation, which for a wing also generates lift as shown in [13]. We show that the difference between laminar and turbulent separation can give rise to non-symmetric separation, which underlies both the *Magnus effect* and the *reverse Magnus effect* generating lift by rotation. We also show that the *Coanda effect* arises from delayed turbulent separation with slip. We start recalling some critcism of Prandtls boundary layer theory.

We compute solutions of the Navier-Stokes equations with *slip/small friction boundary condition* as a model of a turbulent boundary layer, motivated in more detail in [16], using an adaptive finite element method with duality based a posteriori error control described in detail in [14] and referred to as *G2* as an acronym of *General Galerkin*. In particular, the use of slip/small friction boundary condition is justified in [16] by a posteriori analysis. This article relates closely to the new resolution of d'Alembert's paradox and blowup of potential flow [15, 12] and connects to a new analysis of the fluid mechanics of subsonic flight [13]. The entire material is presented to a general audience as Knol articles [17].

4 Can You Prove that Prandtl Was Not Correct?

Lancaster and Birkhoff did not accept Prandtl's explanation of the generation of drag and lift as an effect of a vanishingly small viscosity. But you cannot directly prove that an infinitely small cause cannot have a large effect, without access to an infinitely precise mathematical model or laboratory, which are not available. So Prandtl can be pretty safe to direct attacks, but not to indirect: Suppose you eliminate that vanishingly small cause from the consideration altogether, and yet obtain good correspondence between theory and experiment, that is, suppose you observe the effect without the infinitely small cause. Then you can say that the small cause has little to do with the effect.

This is what we do: We compute turbulent solutions of the incompressible Navier-Stokes equations with *slip* boundary conditions, requiring only the normal velocity to vanish letting the tangential velocity be free, and we obtain drag and lift which fit

with experiments. We thus obtain the effect (drag and lift) without Prandtl's cause consisting of a viscous boundary layer with *no-slip* boundary condition requiring also the tangential velocity to vanish. We conclude that the origin of drag and lift in slightly viscous flow, is not viscous boundary layers with no-slip boundary conditions.

5 Turbulent Separation with Slip/Small Friction

We motivate the use of slip boundary condition by the fact that the *skin friction* of a turbulent boundary layer (the tangential force from a no-slip boundary condition), tends to zero with the viscosity, which is supported by both experiment and computation, also indicating that boundary layers in general are turbulent. More generally, we use a friction-force boundary condition as a model of the skin friction effect of a turbulent boundary layer, with a (small) friction coefficient determined by the *Reynolds number* $Re = \frac{UL}{\nu}$, where U is a representative velocity, L a length scale and ν the viscosity. The limit case of zero friction with slip then corresponds to vanishing viscosity/very large Reynolds number, while large friction models no-slip of relevance for small to moderately large Reynolds numbers. In mathematical terms we combine the Navier-Stokes equations with a natural (Neumann/Robin type) boundary condition for the tangential stress, instead of an essential (Dirichlet type) condition for the tangential velocity as Prandtl did.

We thus make a distinction between laminar separation from a laminar boundary layer with no-slip velocity boundary condition considered by Prandtl, and turbulent separation from a turbulent boundary layer modeled by a slip/small friction boundary condition.

We find quantitative evidence in benchmark problems that the effect on mean-value outputs such as lift and drag of modeling a turbulent boundary layer with a slip/small friction boundary condition, is small in the case of small viscosity. We do this by an a posteriori sensitivity analysis by computational solution of a dual problem linearized at a turbulent solution with no-slip and discovering that relevant stability factors are of moderate size, which we understand to be an effect of cancellation in a turbulent boundary layer, as in the case of interior turbulence studied in [14].

On the other hand, we find linearizing at a laminar solution that corresponding stability factors are large, which indicates that a laminar boundary layer cannot be modeled by slip even if the skin friction is small. However, after laminar separation slightly vicous flow typically turns turbulent which can allow *reattachment* with a turbulent boundary layer.

Altogether, we find that slightly viscous flow in many cases can be modeled by slip/small friction boundary condition with a posteriori justification of the use of slip/small friction boundary conditions.

6 Separation vs Normal Pressure Gradient

Fluid particles with non-zero tangential velocity can only separate from a smooth boundary tangentially, because the normal velocity vanishes on the boundary. By ele-

mentary Newtonian mechanics it follows that fluid particles follow the curvature of the boundary without separation if

$$\frac{\partial p}{\partial n} = \frac{U^2}{R} \tag{1}$$

and separate tangentially if

$$\frac{\partial p}{\partial n} < \frac{U^2}{R}, \tag{2}$$

where p is the pressure, n denotes the unit normal pointing into the fluid, U is the tangential fluid speed and R is the radius of curvature of the boundary counted positive if the body is convex. This is because a certain pressure gradient normal to the boundary is required to accelerate fluid particles to follow the curvature of the boundary.

We understand that flow separation is directly related to the pressure gradient normal to the boundary accelerating fluid particles in the normal direction, while Prandtl instead makes a connection to an adverse pressure gradient retarding the flow in a tangentially to the boundary. We exhibit the difference in several examples below.

7 Laminar Separation with No-Slip

The classical (stationary) *2d boundary layer equations for laminar viscous flow* proposed by Prandtl in 1904 [22], take the following form assuming that the fluid occupies the half plane $x_2 \geq 0$ with main flow in the positive x_1-direction with $u_3 = 0$: Find (u_1, u_2, p) such that

$$\begin{aligned} u_1\frac{\partial u_1}{\partial x_1} + u_2\frac{\partial u_1}{\partial x_2} + \frac{\partial p}{\partial x_1} &= \nu\frac{\partial^2 u_1}{\partial x_2^2}, \\ \frac{\partial u_1}{\partial x_1} + \frac{\partial u_2}{\partial x_2} &= 0, \\ \frac{\partial p}{\partial x_2} &= 0, \end{aligned} \tag{3}$$

combined with the no-slip boundary condition $u_1 = u_2 = 0$, where $\nu > 0$ denotes the viscosity. These equations are formally derived form the Navier-Stokes equations assuming ν to be small, that the flow is constant in the x_3-direction and does not vary quickly in the x_1-direction. An important feature of the boundary layer equations is that the pressure is constant in the x_2-direction as expressed by the equation $\frac{\partial p}{\partial x_2} = 0$, resulting from inertial momentum balance in the x_2-direction:

$$\frac{\partial p}{\partial x_2} \approx -u_1\frac{\partial u_2}{\partial x_1} - u_2\frac{\partial u_2}{\partial x_2}, \tag{4}$$

where in particular $u_1\frac{\partial u_2}{\partial x_1}$ is small because $u_1 = 0$ on the boundary by the no-slip condition.

In the converging flow around a convex body before the crest a positive normal pressure gradient satisfying (1) can be balanced by a negative normal gradient of momentum, but not in the diverging flow after the crest. Assuming the plane $x_2 = 0$ is

tangent to the body at the crest at $x_1 = 0$ with the flow in the (positive) x_1-direction, we have $u_2 > 0$ and $\frac{\partial u_2}{\partial x_2} < 0$ before the crest allowing attachment. On the other hand, at the crest $u_2 = 0$ and in the case of no-slip also $u_1 = 0$, which forces $\frac{\partial p}{\partial x_2} = 0$, thus violating (1) and causing separation. A slightly viscous flow with no-slip thus separates on the crest, but can stay attached before.

The form of the boundary layer equations (3) led Prandtl to focus on the role of of the adverse pressure gradient $\frac{\partial p}{\partial x_1}$ in the momentum balance in the streamwise direction, with the goal of associating separation to adverse pressure gradients retarding the flow, thereby discarding the crucial role of the normal derivative $\frac{\partial p}{\partial x_2}$ effectively connected to separation in slightly viscous flow. Of course, an adverse pressure gradient appears in the expanding flow after the crest, but cannot instantly cause separation, as Prandtl would have to claim in the case of separation at the crest.

Prandtl's boundary layer theory propagated by his student Schlichting in the monumental treatise [23] has dominated modern fluid mechanics, but its inherent paradoxes are today being acknowledged by the fluid mechanics community [4].

8 Turbulent Separation with Slip

In the case of slip boundary condition the tangential velocity u_1 in (4) can be positive. Assuming irrotational flow we have $u_1 \frac{\partial u_2}{\partial x_1} = u_1 \frac{\partial u_1}{\partial x_2}$ where now it is possible that $\frac{\partial u_1}{\partial x_2} < 0$ at the crest, thus allowing $\frac{\partial p}{\partial x_2} > 0$ to satisfy (1) and prevent separation by suction, as we will discover in the closer study below.

9 Potential Flow and Non-Separation

To understand 3d turbulent separation with slip, it is instructive to consider *potential flow* which is *stationary, incompressible, irrotational, inviscid flow* with the velocity $u = \nabla\varphi$, where φ is harmonic in the fluid domain and satisfies the slip boundary condition $u \cdot n = \nabla\varphi \cdot n = 0$ on the boundary.

Potential flow can only separate/attach at a stagnation point with $\nabla\varphi = 0$. In 2d flow this follows from the facts that the flow velocity is the gradient of a harmonic function with a level line of the corresponding conjugate function coinciding with the boundary as long as the gradient does not vanish. Streamlines thus follow level lines of the conjugate function which follow the curvature of the boundary, away from stagnation points. This means that potential flow "sticks to the boundary" and can only separate at a stagnation with opposing flows meeting.

In particular, potential flow around a sphere separates at one stagnation point in the rear, and around a circular cylinder along a line of stagnation with one stagnation point in each cross section.

10 The Incompressible Navier-Stokes Equations

We study laminar and turbulent separation in slightly viscous incompressible flow through the *Navier-Stokes equations* for an *incompressible* fluid of unit density with *small viscosity* $\nu > 0$ and *small skin friction* $\beta \geq 0$ filling a volume Ω in $\mathbb{R}^3$ surrounding a solid body with boundary Γ over a time interval $I = [0, T]$: Find the velocity $u = (u_1, u_2, u_3)$ and pressure p depending on $(x, t) \in \Omega \cup \Gamma \times I$, such that

$$\begin{aligned} \dot{u} + (u \cdot \nabla)u + \nabla p - \nabla \cdot \sigma &= f && \text{in } \Omega \times I, \\ \nabla \cdot u &= 0 && \text{in } \Omega \times I, \\ u_n &= g && \text{on } \Gamma \times I, \\ \sigma_s &= \beta u_s && \text{on } \Gamma \times I, \\ u(\cdot, 0) &= u^0 && \text{in } \Omega, \end{aligned} \tag{5}$$

where $\dot{u} = \frac{\partial u}{\partial t}$, u_n is the fluid velocity normal to Γ, u_s is the tangential velocity, $\sigma = 2\nu\epsilon(u)$ is the stress with $\epsilon(u)$ the usual velocity strain, σ_s is the tangential stress, f is a given volume force, g is a given inflow/outflow velocity with $g = 0$ on a non-penetrable boundary, and u^0 is a given initial condition. We notice the skin friction boundary condition coupling the tangential stress σ_s to the tangential velocity u_s with $\beta = \frac{U}{2} c_f$, where $c_f = \frac{2\tau}{U^2}$ is the *skin friction coefficient*, with $\beta = 0$ for slip (and $\beta >> 1$ for no-slip).

Prandtl insisted on using a no-slip velocity boundary condition with $u_s = 0$ on Γ, because his resolution of d'Alembert's paradox hinged on discriminating potential flow by this condition. On the oher hand, with our new resolution of d'Alembert's paradox, relying instead on instability of potential flow, we are free to choose instead a friction force boundary condition, if data is available. Now, experiments show that the skin friction coefficient decreases with increasing Reynolds number Re as $c_f \approx 0.05 \sim Re^{-0.2}$, so that $c_f \approx 0.0005$ for $Re = 10^{10}$ and $c_f \approx 0.005$ for $Re = 10^5$. Accordingly we model a turbulent boundary layer by friction boundary condition with a friction parameter $\beta \approx 0.03 U Re^{-0.2}$.

We are now performing benchmark computations for tabulating values of β (or σ_s) for different values of Re by solving the Navier-Stokes equations with no-slip, and more generally for different values of ν, U and length scale, since the dependence seems to be more complex than simply through the Reynolds number. Early results are reported in [14] with $\sigma_s \approx 0.005$ for $\nu \approx 10^{-4}$ and $U = 1$, with corresponding velocity strain in the boundary layer $10^4 \sigma_s \approx 50$ indicating that the smallest radius of curvature without separation in this case could be expected to be about 0.02.

We show in [14, 12, 15, **?**, **?**] that the Navier-Stokes equations (5) can be solved by a stabilized finite element referred to as *G2* as an acronym for General Galerkin. G2 produces turbulent solutions characterized by substantial turbulent dissipation from the least squares stabilization acting as an automatic turbulence model, reflecting that the Navier-Stokes residual cannot be made small in turbulent regions. G2 has a posteriori error control based on duality and shows output uniqueness in mean-values such as lift and drag [14, 11, 10, 13, **?**]

We find that G2 with slip is capable of modeling slightly viscous turbulent flow with $Re > 10^6$ of relevance in many applications in aero/hydro dynamics, including

flying, sailing, boating and car racing, with hundred thousands of mesh points in simple geometry and millions in complex geometry, while according to state-of-the-art quadrillions is required [19]. This is because a friction-force/slip boundary condition can model a turbulent blundary layer, and interior turbulence does not have to be resolved to physical scales to capture mean-value outputs [14].

The idea of circumventing boundary layer resolution by relaxing no-slip boundary conditions introduced in [14], was used in [2] in the form of weak satisfaction of no-slip, which however misses the main point of using a force condition instead of a velocity condition.

11 Transition to Turbulence vs Separation

We will analyze 3d turbulent separation as a phenomenon of instability of potential flow at stagnation through the linearized equations

$$\begin{array}{rcll} \dot{v} + (u\cdot\nabla)v + (v\cdot\nabla)\bar{u} + \nabla q &=& f - \bar{f} & \text{in } \Omega\times I,\\ \nabla\cdot v &=& 0 & \text{in } \Omega\times I,\\ v\cdot n &=& g-\bar{g} & \text{on } \Gamma\times I,\\ v(\cdot,0) &=& u^0-\bar{u}^0 & \text{in } \Omega, \end{array} \tag{6}$$

where (u,p) and $(\bar{u},\bar{p})$ are two Euler solutions with slightly different data, and $(v,q)\equiv(u-\bar{u},p-\bar{p})$. Formally, with u and $\bar{u}$ given, this is a linear convection-reaction problem for (v,q) with growth properties governed by the reaction term given by the 3×3 matrix $\nabla\bar{u}$. By the incompressiblity, the trace of $\nabla\bar{u}$ is zero, which shows that in general $\nabla\bar{u}$ has eigenvalues with real values of both signs, of the size of $|\nabla u|$ (with $|\cdot|$ som matrix norm), thus with at least one exponentially unstable eigenvalue. In particular there is exponential perturbation growth in regions where the flow is retarding in the streamwise direction.

Alternatively, applying the curl operator $\nabla\times$ to the momentum equation we obtain the vorticity equation

$$\dot{\omega} + (u\cdot\nabla)\omega - (\omega\cdot\nabla)u = \nabla\times f \quad \text{in } \Omega, \tag{7}$$

which is also a convection-reaction equation in the vorticity $\omega=\nabla\times u$ with coefficients depending on u, of the same form as the linearized equation (6), with a sign change of the reaction term. Also the vorticity is thus locally subject to exponential growth with exponent $|\nabla u|$.

The linearized equations (6) and (3) indicate exponential growth of velocity perturbations in retarding flow and of streamwise vorticity in accellerating flow. We identified in [12] a corresponding basic instablity mechanism generating counter-rotating low-pressure streaks of strong streamwise vorticity attaching to the rear of the body allowing separation without stagnation, as well as the associated cost for separation in terms of increased drag.

Note that in classical analysis it is often argued that from the vorticity equation (3), it follows that vorticity cannot be generated starting from potential flow with zero vorticity and $f=0$, which is *Kelvin's theorem*. But this is an incorrect conclusion,

since perturbations of $\bar{f}$ of f with $\nabla \times \bar{f} \neq 0$ must be taken into account, even if $f = 0$. What you effectively see in computations is local exponential growth of vorticity on the body surface in rear retardation and by vortex stretching in accelleration, even if $f = 0$, which is a main route of instability to turbulence as well as separation.

12 Non-Separation in Viscous Flow

For a completeness we consider also the case of viscous flow with viscous terms dominating over convection terms in which case (4) is replaced by

$$\frac{\partial p}{\partial x_2} \approx \nu \frac{\partial^2 u_2}{\partial x_2^2}. \tag{8}$$

In the converging flow before the crest $\frac{\partial^2 u_2}{\partial x_2^2} > 0$ because the flow cannot separate before the crest, and by (approximate) symmetry of the flow pattern in the flow direction in the case of small convection, $\frac{\partial^2 u_2}{\partial x_2^2} > 0$ also in the diverging flow after the crest thus preventing separation. In short, laminar Stokes flow with dominating viscous terms does not separate, but laminar convection-dominated flow does separate, at the crest.

13 Flow around a Cylinder and Sphere

13.1 Potential Flow

We start considering potential flow in $\mathbb{R}^3$ with coordinates $x = (x_1, x_2, x_3)$ around a circular cylinder of unit radius with axis along the x_3-axis, assuming the flow velocity is $(1, 0, 0)$ at infinity, see Fig. 1. Potential flow is constant in the x_3-direction and fully

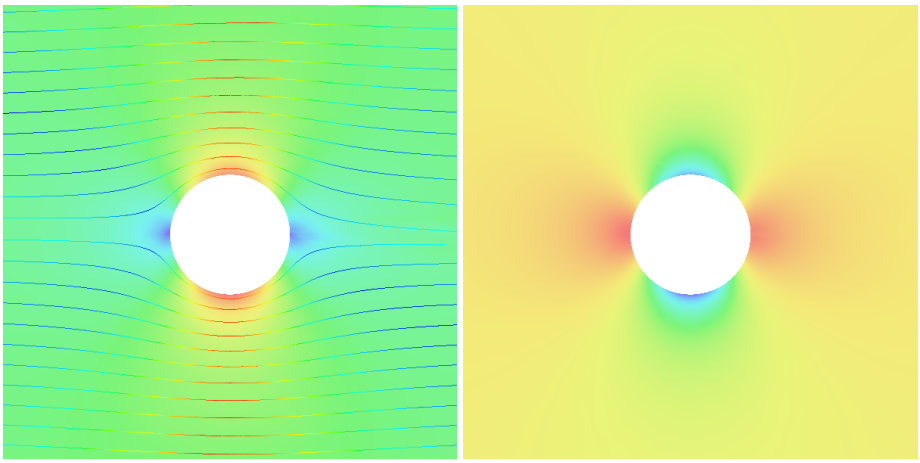

Figure 1: Potential flow past a circular cylinder: velocity (left) and pressure (right).

symmetric in x_1 and x_2, with zero drag/lift and separates at the plane of stagnation

$x_2 = 0$ in the rear. It is given (in polar coordinates (r, θ) in a (x_1, x_2)-plane) by the potential function

$$\varphi(r,\theta) = (r + \frac{1}{r})\cos(\theta)$$

with corresponding velocity components

$$u_r \equiv \frac{\partial \varphi}{\partial r} = (1 - \frac{1}{r^2})\cos(\theta), \quad u_s \equiv \frac{1}{r}\frac{\partial \varphi}{\partial \theta} = -(1 + \frac{1}{r^2})\sin(\theta)$$

with streamlines given as the level lines of the conjugate potential function

$$\psi \equiv (r - \frac{1}{r})\sin(\theta).$$

By Bernouilli's principle the pressure is given by

$$p = -\frac{1}{2r^4} + \frac{1}{r^2}\cos(2\theta)$$

when normalized to vanish at infinity. We compute

$$\frac{\partial p}{\partial \theta} = -\frac{2}{r^2}\sin(2\theta)), \quad \frac{\partial p}{\partial r} = \frac{2}{r^3}(\frac{1}{r^2} - \cos(2\theta)),$$

and discover an adverse pressure gradient in the back, while the normal pressure gradient

$$\frac{\partial p}{\partial r} = 4\sin^2(\theta) \geq 0$$

is precisely the force required to accelerate fluid particles with speed $2|\sin(\theta)|$ to follow the circular boundary without separation, satisfying the condition (1). We note, coupling to the above discussion relating to (4), that $\frac{\partial u_s}{\partial r} = \frac{2}{r^3}\sin(\theta) = 2$ at the crest. We further compute

$$\frac{\partial \psi}{\partial r} = \frac{1}{r^2}\sin(\theta)$$

which shows that fluid particles decrease their distance to the boundary in front of the cylinder and increase their distance in the rear, but the flow only separates at rear stagnation.

13.2 3d Turbulent Separation and Drag Crisis

We find that EG2 solutions with slip initialized as potential flow develop into time-dependent flow with a turbulent wake with counter-rotating low-pressure rolls of streamwise vorticity generating substantial drag, as displayed in Fig. 2 and 3.

We may compare with EG2 computations reported in [**?**, **?**] with variable friction coefficient β. If $\beta > 0.02$ the effect is no-slip with laminar separation at the crest with a drag coefficient $c_D \approx 0.7$. If $\beta < 0.002$, then the effect is slip with $c_D \approx 0.4$. Varying the friction parameter we can thus simulate the *drag crisis* with a drastic reduction of drag due to a switch from laminar separation at the crest to delayed turbulent separation with increasing large Reynolds numbers (in the range $10^5 - 10^6$.)

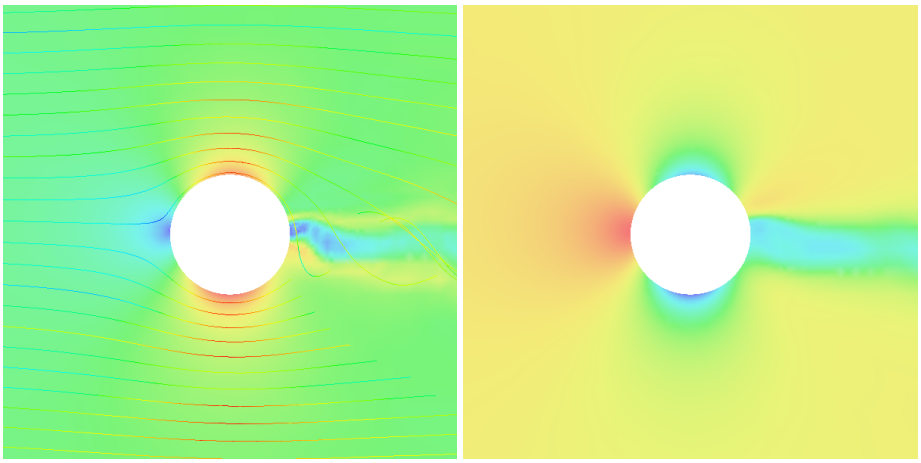

Figure 2: Turbulent flow past a cylinder; velocity (left) and pressure (right). Notice the low pressure wake of strong streamwise vorticity generating drag.

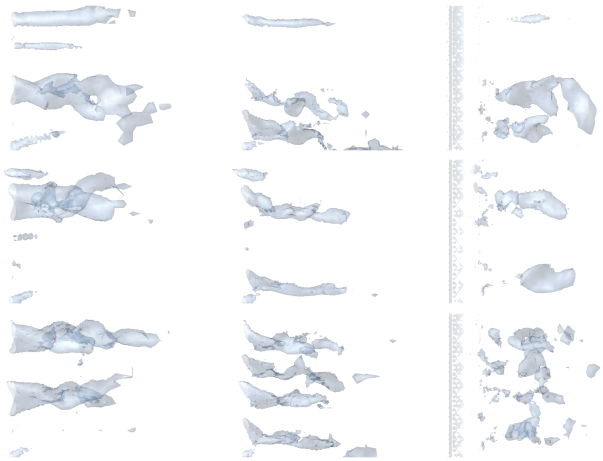

Figure 3: Levels surfaces of strong vorticity in EG2 solution: streamwise $|\omega_1|$ (left) and transversal $|\omega_2|$ (middle) and $|\omega_3|$ (right), at three times $t_1 < t_2 < t_3$ (upper, middle, lower), in the x_1x_3-plane.

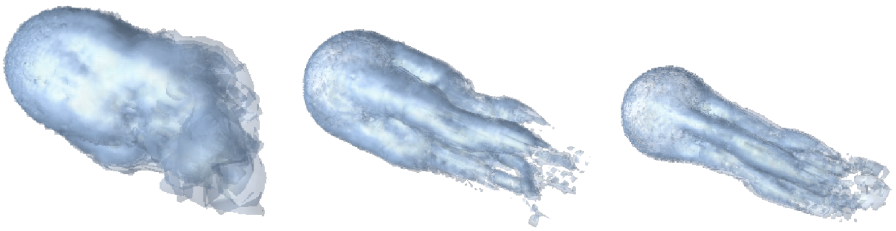

Figure 4: xx

Figure 5: xx

We display similar results for the flow around a sphere from [7] in Fig 4 with $\beta = 2, 10^{-2}, 10^{-2}, 5, 10^{-3}$, with a corresponding drop of drag from 0.5 to 0.2, showing for small friction a pattern of four low-pressure co-rotating streaks of streamwise vorticity which are analogous to the pattern of streamwise streaks behind the cylinder. This indicates that the drag-reducing effect of the dimples of a golf ball is by triggering turbulent separation.

13.3 Separation vs Normal Pressure Gradient

We show in Fig. 5 the normal pressure gradient $\frac{\partial p}{\partial n}$ on the boundary for different patterns of separation varying with the friction, and notice as expected that tangential separation coincides with small $\frac{\partial p}{\partial n}$ (but is not related to an adverse pressure gradient).

EG2 with variable friction thus opens to computational simulation of high Reynolds number flow without resolving thin boundary layers, with potentiall very many applications, considered impossible in state-of-the-art [19].

14 Scenario for 3d Turbulent Separation

We now present a scenario 3d turbulent separation based on identifying 3d perturbations of strong growth in the linearized equations (6) and (3), which consist of low-pressure tubes of streamwise vorticity allowing 3d separation without retardation to

stagnation.

As a basic model of 2d laminar separation we consider the potential flow $u(x) = (x_1, -x_2, 0)$ in the half-plane $\{x_1 > 0\}$ with stagnation at $(0, 0, 0)$ and

$$\frac{\partial u_1}{\partial x_1} = 1 \quad \text{and} \quad \frac{\partial u_2}{\partial x_2} = -1, \tag{9}$$

expressing that the fluid is *squeezed* by *retardation/compression* in the x_2-direction and *accelleration/stretching* in the x_1-direction. We first focus on the compression with the main stability feature of (6) captured in the following simplified version of the v_2-equation, assuming x_1 and x_2 are small, of (6) by

$$\dot{v}_2 - v_2 = f_2,$$

where we assume $f_2 = f_2(x_3)$ to be an oscillating mesh residual perturbation depending on x_3, for example $f_2(x_3) = h\sin(x_3/\delta)$ with $\delta > 0$ expecting the amplitude of f_2 to decrease with δ. We conclude, assuming $v_2(0, x) = 0$, that

$$v_2(t, x_3) = t\exp(t)f_2(x_3).$$

We next turn to the stretching and then focus on the ω_1-vorticity equation, for x_2 small and $x_1 \geq \bar{x}_1 > 0$ with $\bar{x}_1$ small, approximated by

$$\dot{\omega}_1 + x_1\frac{\partial \omega_1}{\partial x_1} - \omega_1 = 0,$$

with the "inflow boundary condition"

$$\omega_1(\bar{x}_1, x_2, x_3) = \frac{\partial v_2}{\partial x_3} = t\exp(t)\frac{\partial f_2}{\partial x_3}.$$

The equation for ω_1 thus exhibits exponential growth, which is combined with exponential growth of the "inflow condition". We can see these features in principle in Fig. 6 and in computational simulation in Fig. **??** showing how opposing flows at separation generate a pattern of alternating surface vortices from pushes of fluid up/down, which act as initial conditions for vorticity stretching into the fluid generating tubes of low-pressure alternating streamwise vorticity.

We thus find streamwise vorticity generated by a force perturbation oscillating in the x_3 direction, which in the retardation of the flow in the x_2-direction creates exponentially increasing vorticity in the x_1-direction, which acts as inflow to the ω_1-vorticity equation with exponential growth by vortex stretching. Thus, we find exponential growth at rear separation in both the retardation in the x_2-direction and the accelleration in the x_1 direction, as a result of the squeezing expressed by (9).

Since the combined exponential growth is independent of δ, it follows that large-scale perturbations with large amplitude have largest growth, which is also seen in computations with δ the distance between streamwise rolls as seen in Fig. 3 which does not seem to decrease with decreasing h. The perturbed flow with swirling separation is large scale phenomenon, which we show below is more stable than potential flow.

The corresponding pressure perturbation changes the high pressure at separation into a zig-zag alternating more stable pattern of high and low pressure with high pressure zones deviating opposing flow into non-opposing streaks which are captured by low pressure to form rolls of streamwise vorticity allowing the flow to spiral away from the body. This is similar to the vortex formed in a bathtub rain.

Notice that at forward separation the retardation does not come from opposing flows, and the zone of exponential growth of ω_2 is short, resulting in much smaller perturbation growth than at rear separation.

The tubes of low-pressure streamwise vorticity change the normal pressure gradient to allow separation without stagnation, but the price is generation of drag as a "cost of separation".

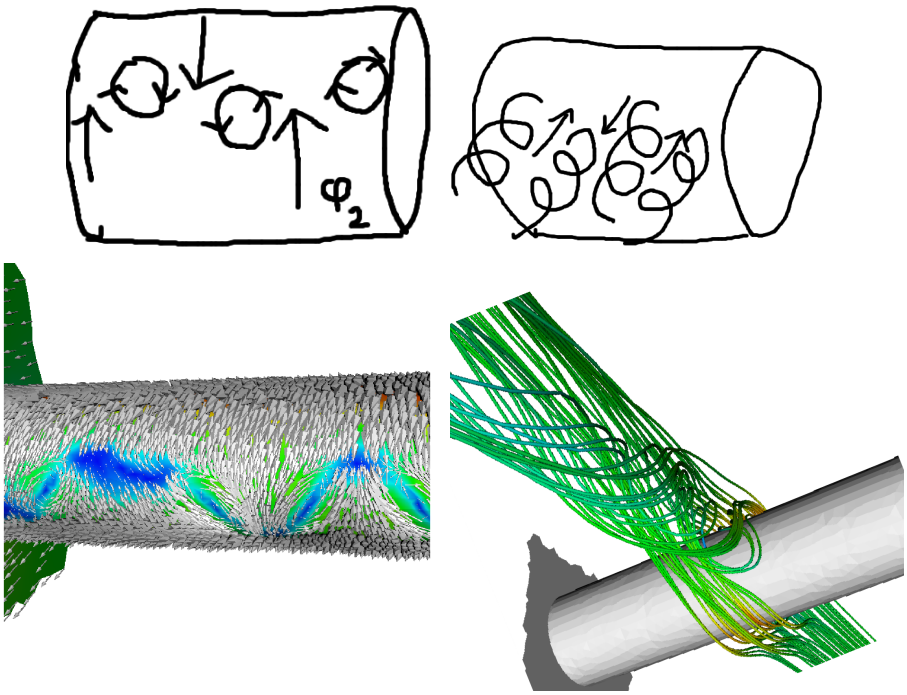

Figure 6: 3d separation in principle and computation

15 Stability of Swirling Separation

A swirling flow with flow velocity $u = (0, x_3, -x_2)$ is stable because the corresponding linearized problem

$$\dot{v}_1 = 0, \quad \dot{v}_2 + v_3 = 0, \quad \dot{v}_3 - v_2 = 0, \tag{10}$$

models a harmonic oscillator without exponential growth.

Overlaying this flow on potential flow, we obtain the following model for swirling flow separation from the halfplane $x_1 > 0$:

$$u = (2\epsilon x_1, x_3 - \epsilon x_2, -x_2 - \epsilon x_3), \tag{11}$$

where $\epsilon > 0$ is a parameter which can be allowed to be small while still allowing fluid particles to separate from the boundary $x_1 = 0$. This is because in swirling flow more time is alloted for separation, since fluid particles spiral away from the boundary. Swirling flow separation thus is a more stable gentle way of separation as compared to unstable more brutal potential flow separation with velocity field $u = (x_1, -x_2, 0)$. Evidently, Nature prefers an elegant stable solution before a brutal unstable. A swirling hand gesture at separation was also practiced in royal courts as an expression of elegance.

The essential problem faced by the flow is how to redirect opposing flows at separation: Potential flow offers a solution, but it is unstable and cannot be realized physically. The instablity results from quick retardation to small speed, redirection followed by quick accelleration, which develops a zig-zag pattern of counterrotating rolls of streamwise vorticity redirecting the flow without retardation to small velocity in opposing flows.

We can compare with the swirling flow in a bathtub drain, which is more stable than fully radial flow. Similarly, capturing a ball with flat hands opposing the ball requires fast action, while allowing the ball to sink into the palm before retarding it gives more time and thus is safer.

16 Applications

16.1 The Magnus effect

Observations show that a top-spin tennis ball curves down, and a backspin curves up, as a result of the *Magnus effect* creating a lift force perpendicular to the flow. For top-spin this can be explained as an effect of non-symmetrical separation occurring because the friction on top of the ball is larger than below, because the relative velocity is larger, and thus the separation occurs later below with a corresponding increase of tangential velocity and pressure drop, resulting in a downward force. Similarly, a back-spin ball curves up because of a delayed separation on top. In G2 we can model this effect by varying the skin friction and thereby obtain non-symmetric separation with lift see [**?**]. In classical fluid mechanics the Magnus effect is described as an effect of large scale rotation of air around a spinning ball, while today the true reason is expected to be non-symmetric separation, which is confirmed by G2 computation.

16.2 The Reverse Magnus Effect

Observations show that a ping-pong ball with strong backspin can curve down seemingly subject to a *reverse Magnus effect*. This can be again be understood as a result of an non-symmetric separation, but this time as an effect of laminar separation at lower

Reynolds number on top because of lower relative speed, and delayed turbulent separation below because of a higher relative speed and higher effective Reynolds number. Computations with no-slip boundary condition above and slip below, confirm this scenario [**?**].

16.3 The Coanda Effect

Holding a spoon vertically under a water faucet, shows the *Coanda effect* of a stream of fluid staying attached to a convex surface. The principle was named after Romanian discoverer Henri Coanda, who was the first to understand the practical importance of the phenomenon in aircraft development, and patented several devices such as the *Coanda saucer*. It is commonly believed that the Coanda effect arises from surface tension or Van der Waals forces, but in the new scenario it is instead seen to be a direct consequence of the tendency of turbulent incompressible Euler flow with slip to stick to a solid boundary.

16.4 Principle of Gliding Flight

The new scenario for flow separation also gives a new explanation of the generation of the lift of a wing, which is fundamentally different from the commonly aacepted explanation by Kutta-Zhukovsky coupling lift to large scale circulation around the wing. We show in [13, 14] that lift is generated by the same mechanism generating drag for a cylinder, which changes the pressure distribution of zero-lift potential flow. We thus show that there is no lift without drag. More precisely we show that low-pressure streamwise vorticity is generated at separation creating both lift and drag [14, 13].

We show in Fig. 7 lift and and drag coefficients of a Naca 0012 3d wing under increasing angles of attack α, as well as the circulation around the wing. We see that the lift increases linearly with α up to 16 degrees, with tangential flow separation on top of the wing starting at 10 degrees and moving upstream from the trailing edge. The lift peaks at stall at $\alpha = 20$ after a quick increase of drag and flow separation at the leading edge. We do not see that the circulation increases with the lift and we conclude that the theory of lift of by Kutta-Zhukovsky is fictional without physical correspondence.

16.5 Turbulent Flow around a Car

In Fig. 8 we show turbulent Euler flow around a car with substantial drag in accordance with wind-tunnel experiments. We see a pattern of streamwise vorticity forming in the rear wake. We also see surface vorticity forming on the hood transversal to the main flow direction.

16.6 Turbulent Flow over a Hill

In Fig. 9 we show turbulent Euler flow over a hill with separation after the crest by again the mechanism of tangential separation through generation of surface vorticity.

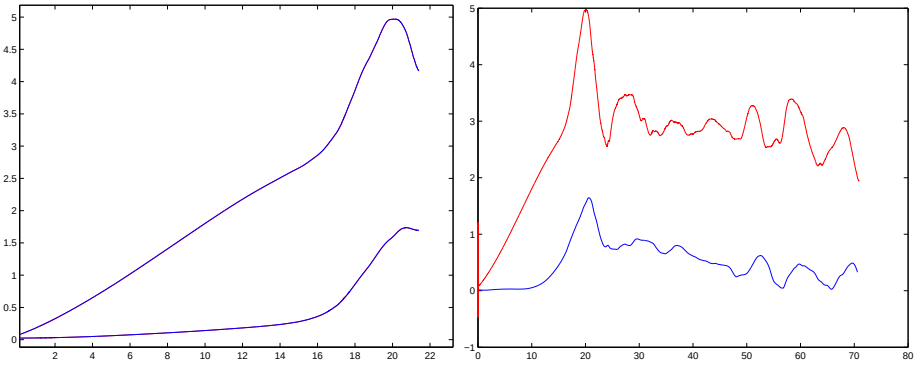

Figure 7: Lift and drag coefficients (left) and lift and circulation (right) as functions of the angle of attack

16.7 Separation into a Turbulent Boundary Layer over a Flat Plate

The experience reported above suggests the following scenario for separation into a turbulent boundary layer over a flat plate as a representation of a smooth boundary: (i) Rolls of streamwise vorticity are formed by non-modal linear perturbation growth referred to as the *Taylor Görtler mechanism* in [14]. (ii) The rolls create opposing transversal flows (as in the back of cylinder), which generate surface vorticity which is stretched into the fluid while being bent into to streamwise direction, as evidenced in e.g. [6, 7].

We note that by energy balance it follows that the total turbulent dissipation in a turbulent boundary layer of width δ_b equals $\sigma_s u_s$ which indicates that $\delta_b \sim \nu^{0.2} U^{0.8}$.

References

[1] John D. Anderson, Ludwig Prandtl's Boundary Layer, http://www.aps.org/units/dfd/resources/upload/prandtlvol58no12p4248.pdf

[2] Y. Bazilevs, C. Michler, V.M. Calo and T.J.R. Hughes, Turbulence without Tears: Residual-Based VMS, Weak Boundary Conditions, and Isogeometric Analysis of Wall-Bounded Flows, Preprint 2008.

[3] G. Birkhoff, Hydrodynamics, Princeton University Press, 1950.

[4] S. Cowley, Laminar boundary layer theory: A 20th century paradox, Proceedings of ICTAM 2000, eds. H. Aref and J.W. Phillips, 389-411, Kluwer (2001).

[5] A. Crook, Skin friction estimation at high Reynolds numbers and Reynolds-number effects for transport aircraft, Center for Turbulence Research, 2002.

[6] A. Ferrante, S. Elghobashi, P. Adams, M. Valenciano, D. Longmire, Evolution of Quasi-Streamwise Vortex Tubes and Wall Streaks in a Bubble-Laden Turbulent Boundary Layer over a Flat Plate, Physics of Fluids 16 (no.9), 2004.

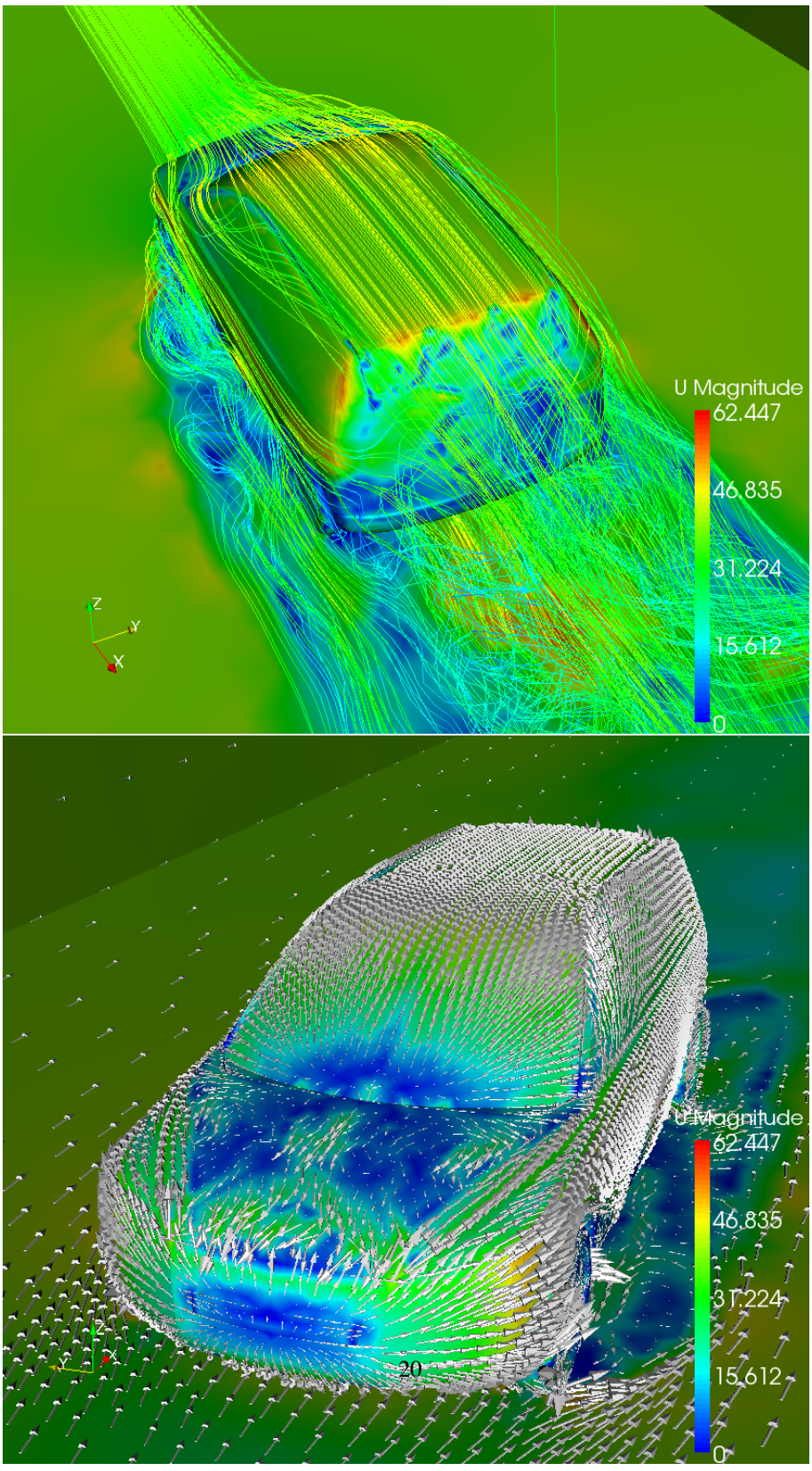
U Magnitude
62.447
46.835
31.224
15.612
0
Z
Y
X
U Magnitude
62.447
46.835
31.224
15.612
0
20

Figure 8: xx

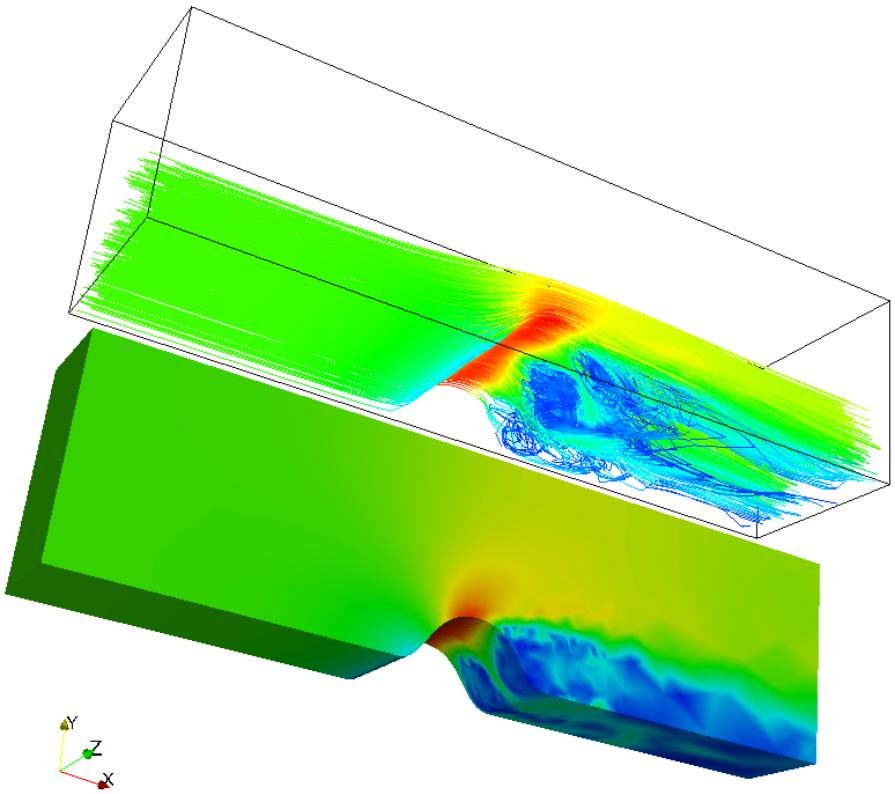

Figure 9: xx

[7] A. Ferrante and S. E. Elghobashi, A robust method for generating inflow conditions for direct numerical simulations of spatially-developing turbulent boundary layers, J. Comp. Phys., 198, 372-387, 2004.

[8] J.Hoffman, Simulation of turbulent flow past bluff bodies on coarse meshes using General Galerkin methods: drag crisis and turbulent Euler solutions, Comp. Mech. 38 pp.390-402, 2006.

[9] J. Hoffman, Simulating Drag Crisis for a Sphere using Friction Boundary Conditions, Proc. ECCOMAS, 2006.

[10] J. Hoffman, Lift and drag of a delta wing by EG2.

[11] J. Hoffman, Drag and lift of a car by EG2.

[12] J. Hoffman and C. Johnson, Blowup of Euler solutions, BIT Numerical Mathematics, Vol 48, No 2, 285-307.

[13] J. Hoffman and C. Johnson, Mathematical Theory of Flight, 2009.

[14] J. Hoffman and C. Johnson, Computational Turbulent Incompressible Flow, Springer 2007, home page at www.bodysoulmath.org/books.

[15] J. Hoffman and C. Johnson, Resolution of d'Alembert's paradox, Journal of Mathematical Fluid Mechanics, Online First Dec 10, 2008.

[16] J. Hoffman and C. Johnson, Modeling Turbulent Boundary Layers by Small Friction.

[17] J. Hoffman and Claes Johnson, Knol articles.

[18] K. Stewartson, D'Alembert's Paradox, SIAM Review, Vol. 23, No. 3, 308-343. Jul., 1981.

[19] J. Kim and P. Moin, Tackling Turbulence with Supercomputer, Scientific American.

[20] F. W. Lancaster, *Aerodynamics*, 1907.

[21] Article in Ny Teknik.

[22] L. Prandtl, On Motion of Fluids with Very Little Viscosity, Third International Congress of Mathematics, Heidelberg, 1904.

[23] H. Schlichting, Boundary Layer Theory, McGraw-Hill, 1979.

[24] James J. Stoker, Bul.l Amer. Math Soc.

[25] D. You and P. Moin, Large eddy simulation of separation over an airfoil with synthetic jet control, Center for Turbulence Research, 2006.